Structure of a Mercaptan–Thermolysin Complex Illustrates Mode of Inhibition of Zinc Proteases by Substrate-Analogue Mercaptans†

A. F. Monzingo and B. W. Matthews*

ABSTRACT: The structure of the complex of thermolysin and the inhibitor (2-benzyl-3-mercaptopropanoyl)-L-alanylglycinamide has been determined by X-ray crystallography at a resolution of 1.9 Å and refined to a crystallographic residual of 18.4%. The binding of this potent, specific inhibitor to thermolysin (K_i = 7.5 × 10^{-7} M) serves as a model for the inhibition of zinc peptidases by substrate-analogue mercaptans. The study shows that the mercaptan inhibitor binds to thermolysin with the sulfur, presumably in the anionic form, tetrahedrally coordinated to the zinc and displacing a water molecule bound to the native enzyme. This is the first direct determination of the mode of binding of a mercaptan inhibitor to a zinc peptidase and confirms the geometry of binding expected on general grounds [Ondetti, M. A., Condon, M. E., Reid, J., Sabo, E. F., Cheung, H. S., & Cushman, D. W. (1979) *Biochemistry 18*, 1427–1430; Nishino, N., & Powers, J. C. (1979) *Biochemistry 18*, 4340–4347] and inferred from previous spectroscopic studies [Holmquist, B., & Vallee, B. L. (1979) *Proc. Natl. Acad. Sci. U.S.A. 76*, 6216–6220].

Recently there has been considerable interest in the development of new types of reversible inhibitors for the zinc peptidases (Cushman et al., 1977; Ondetti et al., 1977, 1979; Nishino & Powers, 1979; Patchett et al., 1980; Harris et al., 1981; Maycock et al., 1981). The progress that has been made is in part due to a better understanding of the functional requirements of a good inhibitor, in part due to the realization that these requirements are common to the different zinc peptidases so that a known inhibitor of one enzyme can be adapted to meet the specificity requirements of the other enzymes, and in part because of the physiological importance of this class of enzymes. The known zinc peptidases include the digestive enzymes carboxypeptidases A and B, collagenase, believed to be the destructive agent in arthritis (Harris & Krone, 1974), the angiotensin-converting enzyme, which is important in the control of blood pressure (Peach, 1977), and the neutral proteases such as thermolysin and *Escherichia coli* neutral protease, which have been isolated from various microorganisms [e.g., see Matsubara & Feder (1971)].

Thermolysin is a heat-stable enzyme, M_r 34 600, isolated from *Bacillus thermoproteolyticus*. Its three-dimensional structure has been determined (Matthews et al., 1974, and references cited therein), and a mechanism of action has been proposed based on the crystallographic studies of several thermolysin–inhibitor complexes (Weaver et al., 1977; Kester & Matthews, 1977a; Bolognesi & Matthews, 1979; Holmes & Matthews, 1981). The structure of carboxypeptidase A has also been determined (Quiocho & Lipscomb, 1971). [For recent discussions of the mechanism of carboxypeptidase A, see, for example, Rees et al. (1980, 1981) and Makinen et al. (1979).] Although their overall three-dimensional structures are quite different, carboxypeptidase A and thermolysin have markedly similar geometric arrangements of their respective active sites (Kester & Matthews, 1977b).

The best inhibitors of the zinc peptidases have been designed to include two functional moieties, the first to coordinate the zinc and the second to mimic the natural substrate of the enzyme (Cushman et al., 1977; Ondetti et al., 1977, 1979; Nishino & Powers, 1979; Patchett et al., 1980; Harris et al., 1981; Maycock et al., 1981). In work reported previously we have determined the modes of binding of carboxylate, phosphoramidate, and hydroxamate inhibitors to thermolysin (Bolognesi & Matthews, 1979; Weaver et al., 1977; Holmes & Matthews, 1981). In this communication, we describe the mode of binding to thermolysin of mercaptan inhibitors. The inhibitor studied in most detail, namely, (2-benzyl-3-mercaptopropanoyl)-L-alanylglycinamide (BAG) (Figure 1), inhibits thermolysin with a K_i of 7.5 × 10^{-7} M (Nishino & Powers, 1979). It is shown that the inhibitor binds to the enzyme with the sulfur, presumably in the anionic form, tetrahedrally coordinated to the zinc. This is the first direct determination of the mode of binding of a mercaptan inhibitor to a zinc peptidase and, as such, provides a model for the other zinc peptidases. The results confirm the geometry of binding inferred from spectroscopic studies of the binding of mercaptans to cobalt-substituted thermolysin (Holmquist & Vallee, 1979).

Materials and Methods

Thermolysin was obtained from Calbiochem and crystallized as described by Colman et al. (1972). The crystals are generally stored in a mother liquor consisting of 0.01 M calcium acetate, 0.01 M tris(hydroxymethyl)aminomethane (Tris)–acetate, and 7% dimethyl sulfoxide (v/v), pH 7.2.

For the purpose of binding the mercaptan inhibitors, which are inactive if oxidized, the thermolysin crystals were equilibrated with mother liquor that also contained 4 mM dithiothreitol. The inhibitor, dissolved in the mother liquor plus dithiothreitol, was added to a vial containing equilibrated native crystals. Some cracking of the crystals did occur, and a soaking concentration was chosen that would minimize cracking but still allow complete, or nearly complete, occupancy of the active site. Binding of the inhibitor was monitored by calculating (*h0l*) difference Fourier projections from precession films [cf. Weaver et al. (1977)]. These preliminary experiments were used to study the binding of two different mercaptans, one the carboxypeptidase-specific inhibitor 2-benzyl-3-mercaptopropanoic acid, a gift of Dr. M. Ondetti (Ondetti et al., 1979), and the other the thermolysin-specific inhibitor BAG, a gift of Dr. J. Powers (Nishino & Powers,

† From the Institute of Molecular Biology and the Department of Physics, University of Oregon, Eugene, Oregon 97403. *Received January 5, 1982.* This work was supported in part by the National Science Foundation (PCM 8014311), by the National Institutes of Health (GM 20066), and by a grant from the M. J. Murdock Charitable Trust.

0006-2960/82/0421-3390$01.25/0

Table I: Intensity Statistics

films	28
av R_{sym}[a]	0.079
av R_{sca}[a]	0.051
R_{merge}[a]	0.116
av isomorphous difference (%)	11.7
reflections	20919

[a] $R = \Sigma|I - \bar{I}|/\Sigma\bar{I}$. R_{sym} measures the agreement between symmetry-related reflections recorded on the same film, R_{sca} gives the agreement between reflections measured on successive films in a film pack, and R_{merge} gives the overall agreement between reflections measured on different films.

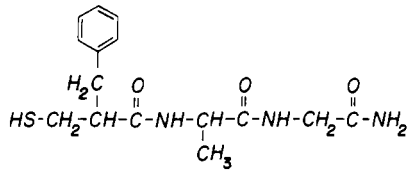

FIGURE 1: Chemical formula of the mercaptan inhibitor (2-benzyl-3-mercaptopropanoyl)-L-alanylglycinamide.

1979). In each case the difference electron density projection indicated that the sulfur atom was probably liganded to the zinc.

Since the geometry of binding is presumably similar for the two inhibitors, a full three-dimensional high-resolution study was carried out only for the thermolysin-specific mercaptan. Two crystals soaked in the same vial for 6 days with 45 μM BAG sufficed for three-dimensional data collection. Data were collected to 1.9-Å resolution by using oscillation photography (Schmid et al., 1981). An oscillation angle of 1.2°/film pack was used, and the crystals, space group $P6_122$, were rotated about the c axis through a net rotation of 30°. The X-ray source was a graphite-monochromatized GX-21 rotating anode generator operated at 39 kV, 130 mA, and the exposure time was 6 h/film pack. Intensity statistics are summarized in Table I.

Results

Modeling Electron Density of Inhibitor. A difference electron density map calculated with amplitudes ($F_{inhib} - F_{nat}$) and with phases determined by multiple isomorphous replacement (Matthews et al., 1974) showed that the inhibitor was bound to the protein in the active site region, but because of the displacement of bound solvent molecules, the map was not suitable for model building [cf. Kester & Matthews (1977a)]. The difference map had a large peak (height 6σ) in the vicinity of the zinc ion, corresponding to the sulfur atom, and other features (5σ–6σ) in the active site region, corresponding to other parts of the inhibitor. An electron density map with amplitudes ($2F_{inhib} - F_{nat}$) was calculated (Figure 2), and a brass model (Cambridge Repetition Engineers) of the inhibitor was fit to the electron density in an optical comparator (Richards, 1968; Colman et al., 1972). Markers corresponding to each atom were placed in the map by using the brass model as a guide and served to provide approximate coordinates for the bound inhibitor.

Refinement of Protein–Inhibitor Complex. The coordinates of the inhibitor–protein complex were refined to a crystallographic residual of 18.4% by using the energy minimization and crystallographic refinement program of Jack & Levitt (1978). The starting parameters were the approximate inhibitor coordinates together with coordinates of native thermolysin and bound water molecules, which had been refined at 2.3-Å resolution by using the restrained least-squares re-

Table II: Refinement Statistics

resolution (Å)	1.9
initial R factor (20.0–1.9 Å) (%)	25.2
final R factor (%)	18.4
no. of cycles	20
no. of reflections used	20808
no. of atoms	2604

Table III: Deviation from "Ideal" Geometry

	protein-inhibitor complex		inhibitor	
	no.	rms deviation	no.	rms deviation
bond length	2513	0.026 Å	22	0.033 Å
bond angle	3412	3.6°	28	5.3°
planarity (trigonal)	66	0.071 Å		
planarity (other planes)	378	0.048 Å	4	0.058 Å

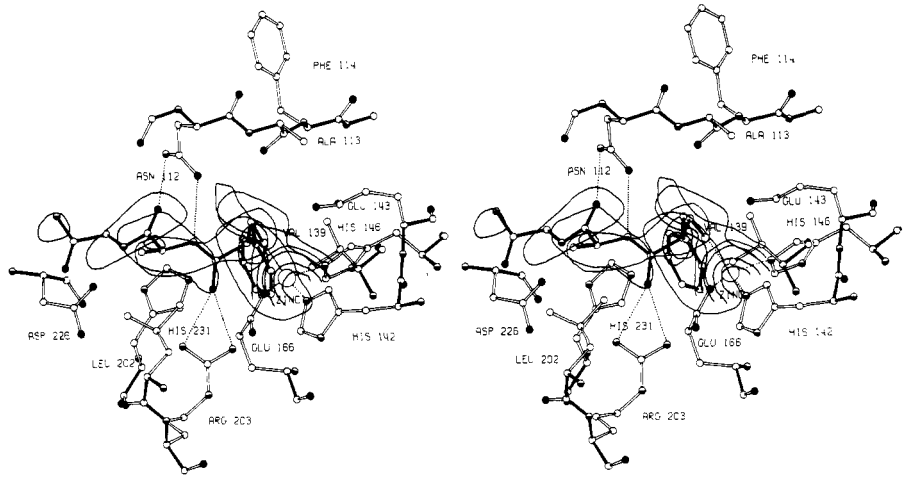

FIGURE 2: Stereo drawing of the refined structure of BAG bound in the active site region of thermolysin superimposed on an electron density map calculated with amplitudes ($2F_{inhib} - F_{nat}$) and phases to 2.3-Å resolution determined by multiple isomorphous replacement. Contours are drawn at levels 1, 3, and 5 times the standard deviation of the map. Only the density that we believe to correspond to the inhibitor and part of the zinc is shown. Carbon atoms are drawn open, oxygen atoms solid, and nitrogen atoms half-solid. Contacts between the inhibitor and the protein believed to be hydrogen bonds (less than 3.1 Å) and contacts between the zinc and its liganding atoms are displayed by dotted lines. The glycinamide region of the inhibitor displays weak electron density as might be expected since it is likely weakly bound, having no hydrogen-bonding contacts with the protein.

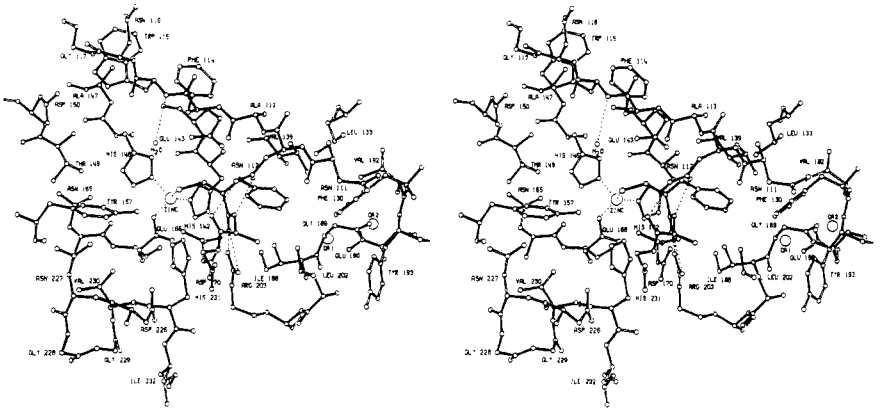

FIGURE 3: Stereo view of BAG bound in active site region of thermolysin. The direction of view is from the left of that shown in Figure 2. Contacts believed to be hydrogen bonds and contacts between the zinc and its ligands are shown by dotted lines.

Table IV: Inhibitor Coordinates[a]

residue	atom	x	y	z	B
ψ-Phe	SG	52.9	19.3	−6.8	27
	CB2	52.1	18.8	−5.3	27
	CD2	52.7	18.1	−0.6	27
	CE2	53.8	18.1	0.3	31
	CZ	55.0	18.6	0.0	35
	CE1	55.2	19.4	−1.2	28
	CD1	54.2	19.4	−2.1	31
	CG	53.0	18.7	−1.8	26
	CB1	52.0	18.6	−2.9	22
	CA	52.9	18.5	−4.0	28
	C	53.7	17.1	−3.9	28
	O	55.0	16.9	−3.9	19
Ala	N	52.9	16.1	−3.8	21
	CB	53.3	13.8	−2.8	21
	CA	53.2	14.7	−4.0	31
	C	52.4	14.2	−5.2	34
	O	51.4	14.7	−5.7	26
Gly	N	53.1	13.1	−5.6	34
	CA	52.5	12.4	−6.7	40
	C	52.8	11.0	−6.5	40
	O	54.0	10.6	−6.5	33
	N	51.7	10.2	−6.5	36
H_2O (A)		50.0	20.9	−8.2	34
H_2O (B)		56.7	10.0	−6.7	22

[a] Coordinates are in angstroms in the standard orthogonal thermolysin coordinate frame (Matthews et al., 1974). B is in angstroms squared.

Table V: Zinc-Ligand Geometry

ligand	distance (Å)
His-142 NE2	2.0
His-146 NE2	2.1
Glu-166 OE1	1.8
inhibitor S	1.9
ligands	**angle (deg)**
S-Zn-NE2 (His-142)	119.5
S-Zn-NE2 (His-146)	108.2
S-Zn-OE1 (Glu-166)	98.8

Table VI: Thermolysin-Inhibitor Distances

protein	inhibitor	distance (Å)
Asn-112 OD1	Ala N	3.1
Arg-203 NEE1	ψ-Phe O	2.9
Arg-203 NEE2	ψ-Phe O	2.8
Asn-112 ND2	Ala O	2.9

finement program of Hendrickson & Konnert (1980) (Holmes & Matthews, 1981; M. A. Holmes and B. W. Matthews, unpublished results). Refinement statistics are summarized in Table II, and the deviations from ideal geometry for the refined protein–inhibitor complex and the inhibitor alone are shown in Table III. Refined coordinates of the inhibitor are listed in Table IV. The coordinates of a water molecule (H_2O–A) that is apparently hydrogen bonded to the Trp-115 backbone nitrogen in the active site region and of another water molecule (H_2O–B) hydrogen bonded to the carbonyl oxygen of the inhibitor glycinamide residue are also included. The uncertainty of the refined inhibitor coordinates, estimated by the method of Luzzatti (1952), is approximately 0.3 Å.

Binding of Inhibitor. The observed binding of the inhibitor in the thermolysin active site is shown stereographically in Figures 2 and 3. As expected, the sulfur atom of the inhibitor is coordinated with the zinc as a distorted tetrahedral ligand. The sulfur–metal distance is 1.9 Å. Additional details of the geometry of the zinc ligands are summarized in Table V. As can be seen, the four ligands are all approximately 2.0 Å from the metal, and the geometry is approximately tetrahedral. As observed in previous thermolysin–inhibitor studies, the phenyl

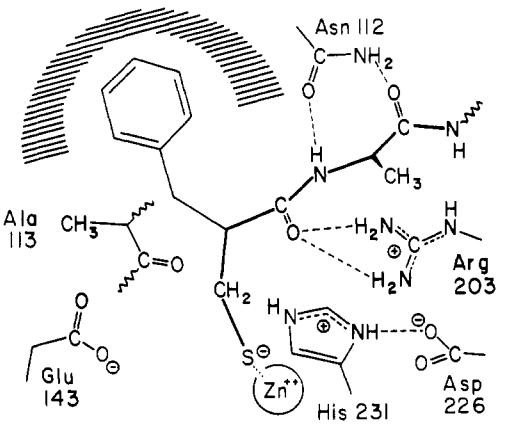

FIGURE 4: Schematic drawing showing the observed mode of binding of the mercaptan inhibitor BAG in the active site region. The pseudophenylalanyl moiety binds in the position of the R_1' residue and the alanyl moiety in the position of the R_2' residue as designated for a model-extended substrate [see Figure 5 in Weaver et al. (1977)].

ring of the inhibitor is bound in the S_1' hydrophobic specificity pocket (Weaver et al., 1977; Kester & Matthews, 1977a; Bolognesi & Matthews, 1979; Holmes & Matthews, 1981).

Table VI lists all the close interatomic contacts between the protein and the inhibitor. The propanoyl carbonyl oxygen of the inhibitor lies within hydrogen-bonding distance of both the NEE1 atom (2.9 Å) and the NEE2 atom (2.8 Å) of Arg-203. A second hydrogen bond, distance 2.9 Å, is apparently formed between the ND2 atom of Asn-112 and the carbonyl oxygen of the inhibitor alanine residue. In modeling the binding of

an extended substrate and of this inhibitor, it has been assumed that the amide nitrogen of the R_2' residue is hydrogen bonded to the OD1 atom of Asn-112 (Figure 4). The refined interatomic distance for this contact is 3.1 Å, somewhat long for a hydrogen bond. On the other hand, since the refined atom positions have a probable accuracy of about 0.3 Å, this still remains as a potential hydrogen bond.

Discussion

In recent years, several authors have discussed a rationale for the design of inhibitors of zinc peptidases in which a moiety that will bind as a ligand to the zinc atom is coupled with a peptide chain that will bind in the active site in a manner similar to that of a substrate. Following this rationale, a series of compounds including a phosphoramide, hydroxamate, carboxyl, or mercaptan function have been synthesized and shown to be good inhibitors of various zinc peptidases (Cushman et al., 1977; Ondetti et al., 1977, 1979; Nishino & Powers, 1979; Holmquist & Vallee, 1979; Patchett et al., 1980; Harris et al., 1981; Maycock et al., 1981). Mercaptan inhibitors have proven to be among the most potent of these, with K_i's approaching 10^{-9} M in some cases. In this communication, we have described the mode of binding to thermolysin of a mercaptan inhibitor that was designed and synthesized according to the above rationale.

It has been anticipated that the mercaptan inhibitors bind to the zinc peptidases with the thiol liganded directly to the metal (Cushman et al., 1977; Ondetti et al., 1977; Nishino & Powers, 1979). In addition, Holmquist & Vallee (1979) have presented spectroscopic evidence indicating that the S^- group coordinates as a fourth metal ligand to cobalt-substituted thermolysin and other zinc proteases. It was inferred that a similar geometry of binding occurs with the native, zinc-substituted enzymes, but because zinc is spectroscopically inert, this could not be proven. The present crystallographic study provides a direct visualization of a mercaptan inhibitor bound in situ and confirms that the mode of binding of these inhibitors is as anticipated (Figure 4). In the mercaptan–thermolysin complex the sulfur atom of the inhibitor binds to the zinc as a fourth tetrahedral ligand, displacing the water molecule that acts as the fourth ligand in the native thermolysin structure. Because the structure of the thermolysin–inhibitor complex has been refined to high resolution (Table II), the geometry is reliable, with an estimated standard error of about 0.3 Å. Tetrahedral coordination to the zinc has also been observed in previous structural studies of thermolysin–inhibitor complexes, for example, the carboxylate group of L-benzylsuccinic acid (Bolognesi & Matthews, 1979) and the phosphinyl group of phosphoramidon (Weaver et al., 1977).

As expected, the mode of binding of the BAG inhibitor also resembles that of a substrate with interactions at the S_1' and S_2' recognition sites. Kinetic data indicate that a hydrophobic amino acid side chain is preferred for binding at the primary recognition site (S_1') (Nishino & Powers, 1979). The R_1' residue of BAG is a pseudophenylalanine, and as seen previously, the phenyl ring of this residue occupies the hydrophobic pocket at the S_1' site of the enzyme. Other interactions involve hydrogen bonds between the inhibitor main chain and protein side chains (Table VI; Figures 2 and 3). The importance of these specific substratelike interactions is indicated by the fact that nonspecific mercaptans such as cysteine and β-mercaptoethanol inhibit thermolysin with a K_i of $\sim$1 mM as opposed to $\sim$1 μM for BAG (Nishino & Powers, 1979; Holmquist & Vallee, 1979).

It can be reasonably inferred that the geometry of binding seen for mercaptans bound to thermolysin also occurs for the other zinc proteases such as carboxypeptidase A and angiotensin-converting enzyme. This would be expected on general grounds, but in addition, we have shown that there is a striking resemblance between the active sites of thermolysin and carboxypeptidase A, not only with respect to corresponding elements of the two proteins but also with respect to the geometry of substrate binding (Kester & Matthews, 1977b). In the case of the inhibitor L-benzylsuccinic acid, which we observed binding to crystalline thermolysin, we used the known geometrical transformation between the two enzymes to predict the location that this inhibitor would occupy when bound to carboxypeptidase A (Bolognesi & Matthews, 1979). A subsequent crystallographic analysis of a structurally analogous inhibitor showed that the predicted position was, indeed, close to that observed (Rees et al., 1980). The important point is not so much that one can transform sets of coordinates from one protein to another but rather that the accuracy of this transformation bespeaks the striking similarity that exists between thermolysin and carboxypeptidase A and possibly between the other zinc peptidases as well. For this reason, we suggest that the results presented here not only apply to thermolysin but also can be taken as a general model for the mechanism of inhibition of all of the zinc peptidases by specific mercaptan inhibitors.

Acknowledgments

We are grateful to Dr. M. A. Ondetti, Squibb Institute for Medical Research, and Dr. J. C. Powers, Georgia Institute of Technology, for gifts of inhibitors, and we thank Drs. L. H. Weaver and M. A. Holmes for advice and assistance in data collection, refinement, and other procedures.

References

Bolognesi, M. C., & Matthews, B. W. (1979) *J. Biol. Chem. 254*, 634.

Colman, P. M., Jansonius, J. N., & Matthews, B. W. (1972) *J. Mol. Biol. 70*, 701.

Cushman, D. W., Cheung, H. S., Sabo, E. F., & Ondetti, M. A. (1977) *Biochemistry 16*, 5484.

Harris, E. D., & Krone, S. M. (1974) *N. Engl. J. Med. 291*, 557, 605, 652.

Harris, R. B., Ohlsson, J. T., & Wilson, I. B. (1981) *Arch. Biochem. Biophys. 206*, 105.

Hendrickson, W. A., & Konnert, J. H. (1980) in *Computing in Crystallography* (Diamond, R., Ramaseshan, S., & Venkatesan, K., Eds.) pp 13.01–13.23, Indian Academy of Sciences, Bangalore, India.

Holmes, M. A., & Matthews, B. W. (1981) *Biochemistry 20*, 6912.

Holmquist, B., & Vallee, B. L. (1979) *Proc. Natl. Acad. Sci. U.S.A. 76*, 6216.

Jack, A., & Levitt, M. (1978) *Acta Crystallogr., Sect. A A34*, 931.

Kester, W. R., & Matthews, B. W. (1977a) *Biochemistry 16*, 2506.

Kester, W. R., & Matthews, B. W. (1977b) *J. Biol. Chem. 252*, 7704.

Luzzatti, P. V. (1952) *Acta Crystallogr. 5*, 802.

Makinen, M. W., Kuo, L. C., Dymowski, J. J., & Jaffer, S. (1979) *J. Biol. Chem. 254*, 356.

Matsubara, H., & Feder, J. (1971) *Enzymes, 3rd Ed. 3*, 721.

Matthews, B. W., Weaver, L. H., & Kester, W. R. (1974) *J. Biol. Chem. 249*, 8030.

Maycock, A. L., De Sousa, D. M., Payne, L. G., ten Broeke, J., Wu, M. T., & Patchett, A. A. (1981) *Biochem. Biophys. Res. Commun. 102*, 963.

Nishino, N., & Powers, J. C. (1979) *Biochemistry 18*, 4340.
Ondetti, M. A., Rubin, B., & Cushman, D. W. (1977) *Science (Washington, D.C.) 196*, 441.
Ondetti, M. A., Condon, M. E., Reid, J., Sabo, E. F., Cheung, H. S., & Cushman, D. W. (1979) *Biochemistry 18*, 1427.
Patchett, A. A., Harris, E., Tristram, E. W., Wyvratt, M. J., Wu, M. T., Taub, D., Peterson, E. R., Ikeler, T. J., ten Broeke, J., Payne, L. G., Ondeyka, D. L., Thorsett, E. D., Greenlee, W. J., Lohr, N. S., Hoffsommer, R. D., Joshua, H., Ruyle, W. V., Rothrock, J. W., Aster, S. D., Maycock, A. L., Robinson, F. M., Hirschmann, R., Sweet, C. S., Ulm, E. H., Gross, D. M., Vassil, T. C., & Stone, C. A. (1980) *Nature (London) 288*, 280.
Peach, M. J. (1977) *Physiol. Rev. 57*, 313.
Quiocho, F. A., & Lipscomb, W. N. (1971) *Adv. Protein Chem. 25*, 1.
Rees, D. C., Honzatko, R. B., & Lipscomb, W. N. (1980) *Proc. Natl. Acad. Sci. U.S.A. 77*, 3288.
Rees, D. C., Lewis, M., Honzatko, R. B., Lipscomb, W. N., & Hardman, K. D. (1981) *Proc. Natl. Acad. Sci. U.S.A. 78*, 3408.
Richards, F. M. (1968) *J. Mol. Biol. 37*, 225.
Schmid, M. F., Weaver, L. H., Holmes, M. A., Grütter, M. G., Ohlendorf, D. H., Reynolds, R. A., Remington, S. J., & Matthews, B. W. (1981) *Acta Crystallogr., Sect. A A37*, 701.
Weaver, L. H., Kester, W. R., & Matthews, B. W. (1977) *J. Mol. Biol. 114*, 119.

Purification of Ornithine Decarboxylase from Kidneys of Androgen-Treated Mice†

James E. Seely,‡ Hannu Pösö,§ and Anthony E. Pegg*

ABSTRACT: Ornithine decarboxylase has been purified to homogeneity from kidneys of androgen-treated mice. Such kidneys have an enzyme content 2 orders of magnitude greater than that of other mammalian tissues such as induced rat liver, and only a 10350-fold purification was needed for purification. The enzyme preparation gave a single band on isoelectric focusing and on polyacrylamide gel electrophoresis under native and denaturing conditions. These bands corresponded to the enzyme activity and to the migration of ornithine decarboxylase labeled by reaction with α-(difluoromethyl)[5-^{14}C]ornithine, a specific inhibitor. The enzyme has a M_r of about 100000 and is a dimer of subunit M_r 53000. The K_m for L-ornithine was 75 μM and for pyridoxal phosphate, 0.3 μM. The preparation had a specific activity of 50 μmol of CO_2 produced min^{-1} mg^{-1} and bound a stoichiometric amount of the irreversible inhibitor, α-(difluoromethyl)ornithine (one molecule per subunit). The purified enzyme was unstable even in the presence of 2.5 mM dithiothreitol and 40 μM pyridoxal phosphate unless 0.02% Brij 35 was added. In the presence of this detergent, the enzyme could be stored with little loss of activity.

There has been considerable interest in the enzyme ornithine decarboxylase (EC 4.1.1.17) for a number of reasons [reviewed by Morris & Fillingame (1974), Jänne et al. (1978), Canellakis et al. (1979), McCann (1980), Russell (1980), and Pegg & Williams-Ashman (1981)]. In mammalian cells, this enzyme provides the only source of putrescine, a precursor of the polyamines. Its activity increases very rapidly in response to a wide variety of trophic stimuli, and it appears to have the most rapid rate of protein synthesis and degradation among mammalian enzymes. Its activity may also be regulated by the level of a macromolecular inhibitor (Canellakis et al., 1978) and a variety of posttranslational modifications (Mitchell, 1981; Russell, 1981; Atmar & Kuehn, 1981). The enzyme is the target for potentially useful chemotherapeutic agents that block polyamine production (Sjoerdsma, 1981; Heby & Jänne, 1981). Despite the intense interest in ornithine decarboxylase, the mammalian enzyme has proved difficult to purify. Homogeneous preparations of ornithine decarboxylase have been obtained in milligram quantities from bacteria (Applebaum et al., 1975, 1977; Guirard & Snell, 1980) and from yeast and slime mold (Tyagi et al., 1981; Atmar & Kuehn, 1981; Mitchell et al., 1978) but not from mammalian tissues. Highly purified preparations have been reported for the enzyme from rat prostate (Jänne & Williams-Ashman, 1971), rat liver (Ono et al., 1972; Obenrader & Prouty, 1977; Pegg & McGill, 1979; Kitani & Fujisawa, 1981), calf liver (Haddox & Russell, 1981), mouse fibroblasts (Weiss et al., 1981), and mouse kidney (Persson, 1981a,b), but convincing evidence that these preparations are homogeneous was not given. In fact, numerous preparations of rat liver ornithine decarboxylase have been published, each describing the purification of a material giving a single band on polyacrylamide gel electrophoresis but increasing the specific activity of the purified material (Friedman et al., 1972; Ono et al., 1972; Hölttä, 1975; Obenrader & Prouty, 1977; Pegg & McGill, 1979; Kitani & Fujisawa, 1981). A recent preparation notes that the material was not homogeneous when tested by isoelectric focusing, although the specific activity of 1 μmol of CO_2 min^{-1} mg^{-1} was greater than those previously published (Kitani

† From the Department of Physiology and Specialized Cancer Research Center, College of Medicine, The Milton S. Hershey Medical Center, The Pennsylvania State University, Hershey, Pennsylvania 17033. *Received February 23, 1982.* This investigation was supported by Grant CA-18138 from the National Institutes of Health.

‡ Recipient of a training fellowship (1 T32 HL-07223) from the National Institutes of Health.

§ Present address: Research Laboratories of the State Alcohol Monopoly (Alko), SF-00707 Helsinki, 10 Finland. Recipient of a research fellowship from the Research Council for Natural Sciences of the Academy of Finland and a travel grant from the League of Finnish American Societies Scholarship Foundation (thanks to a Scandinavian grant).

0006-2960/82/0421-3394$01.25/0